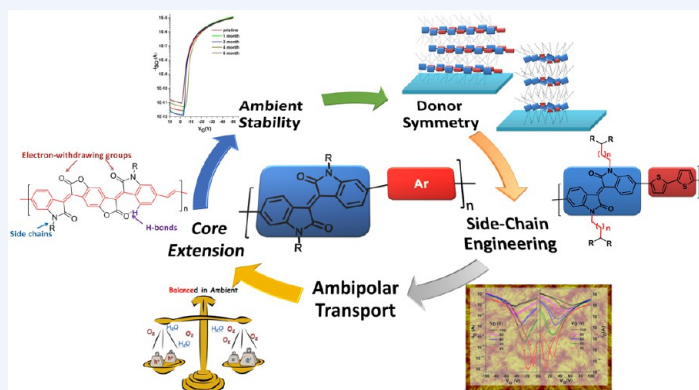


Design, Synthesis, and Structure–Property Relationships of Isoindigo-Based Conjugated Polymers

Ting Lei, Jie-Yu Wang, and Jian Pei*

Beijing National Laboratory for Molecular Sciences, The Key Laboratory of Bioorganic Chemistry and Molecular Engineering of Ministry of Education, College of Chemistry and Molecular Engineering, Peking University, Beijing 100871, China



ABSTRACT: Conjugated polymers have developed rapidly due to their promising applications in low-cost, lightweight, and flexible electronics. The development of the third-generation donor–acceptor (D–A) polymers greatly improved the device performance in organic solar cells (OSCs) and field-effect transistors (FETs). However, for further improvement of device performance, scientists need to develop new building blocks, in particular electron-deficient aromatics, and gain an in-depth understanding of the structure–property relationships.

Recently, isoindigo has been used as a new acceptor of D–A conjugated polymers. An isomer of indigo, isoindigo is a less well-known dye and can be isolated as a by-product from certain biological processes. It has two lactam rings and exhibits strong electron-withdrawing character. This electron deficiency gives isoindigo-based polymers intriguing properties, such as broad absorption and high open circuit voltage in OSCs, as well as high mobility and good ambient stability in FETs.

In this Account, we review our recent progress on the design, synthesis, and structure–property relationship study of isoindigo-based polymers for FETs. Starting with some discussion on carrier transport in polymer films, we provide some basic strategies towards high-performance polymer FETs. We discuss the stability issue of devices, the impediment of the alkyl side chains, and the choice of the donor part of conjugated polymers. We demonstrate that introducing the isoindigo core effectively lowers the HOMO levels of polymers and provides FETs with long-time stability. In addition, we have found that when we use inappropriate alkyl side chains or non-centrosymmetric donors, the device performance of isoindigo polymers suffers. To further improve device performance and ambient stability, we propose several design strategies, such as using farther branched alkyl chains, modulating polymer energy levels, and extending π -conjugated backbones. We have found that using farther branched alkyl chains can effectively decrease interchain π – π stacking distance and improve carrier mobility. When we introduce electron-deficient functional groups on the isoindigo core, the LUMO levels of the polymers markedly decrease, which significantly improves the electron mobility and device stability. In addition, we present a new polymer system called BDOPV, which is based on the concept of π -extended isoindigo. By application of some strategies successfully used in isoindigo-based polymers, BDOPV-based polymers exhibit high mobility and good stability both in n-type and in ambipolar FETs. We believe that a synergy of molecular engineering strategies towards the isoindigo core, donor units, and side chains may further improve the performance and broaden the application of isoindigo-based polymers.

INTRODUCTION

The huge demand for low-cost, lightweight, and flexible electronics continues to drive the development of next-generation electronics. Conjugated polymers have emerged as a class of promising materials due to their good mechanical properties and low-cost high-throughput production.^{1–3} Benefitting from new structural design and improved fabrication processes, significant progress has been made for

polymer semiconductors, both in organic circuitry and in solar cell applications.^{4,5} Recently, donor–acceptor (D–A) polymers have contributed greatly to this development.^{6,7} Several electron-deficient fused aromatic units, such as diketopyrrolopyrrole (DPP), naphthalene diimide (NDI), and benzobisthia-

Received: October 28, 2013

Published: February 6, 2014

diazole (BBT), are extensively used as the acceptor.^{7–9} However, further improvement of the device performance requires the development of new electron-deficient aromatics and the in-depth understanding of the structure–property relationships.

Unlike its famous isomer indigo, isoindigo is a less investigated dye and is isolated as a byproduct from certain biological processes. It has two lactam rings and exhibits strong electron-withdrawing character. Although discovered as a dye over a century ago, isoindigo has joined the “acceptor club” of D–A polymers only recently. Reynolds et al. first used isoindigo in organic solar cells (OSCs) in 2010 to represent the first application of isoindigo in organic electronics.¹⁰ Inspired by this seminal work, our group developed the first isoindigo-based polymer field-effect transistors (FETs).¹¹ Recently, isoindigo-based polymers have attracted increasing attention in the development of conjugated polymers for OSCs and FETs. High power-conversion efficiency over 8%^{12–14} and high mobility over $3 \text{ cm}^2 \text{ V}^{-1} \text{ s}^{-1}$ were successfully achieved.¹⁵

In this Account, we focus on the design, synthesis, and structure–property relationship study of isoindigo-based polymers. Before the discussion of isoindigo-based polymers, some theoretical considerations of charge carrier transport in conjugated polymers are discussed. Furthermore, a new polymer system (BDOPV) based on the concept of π -extended isoindigo is also presented. Photovoltaic properties of isoindigo-based polymers are generally not included, because the mechanism and the process in OSCs are in general more complicated than those in FETs.

■ CHARGE TRANSPORT IN POLYMER FILMS

Charge transport in polymer films generally contains two processes: intrachain and interchain transports (Figure 1a).

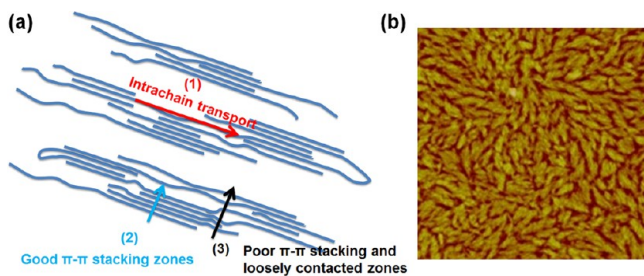


Figure 1. (a) Charge transport process in polymer FETs and (b) typical AFM height image of polymer films.

Intrachain transport (pathway 1 in Figure 1a) is realized by π -electron delocalization along polymer backbones, providing high carrier mobility according to theoretical predictions. The intrachain transport is largely determined by the effective conjugation length of the polymer, which is limited by the torsional disorder along polymer backbone and the presence of chemical defects.¹⁶ Using time-resolved microwave conductivity measurement, the intrachain mobility of a ladder-type poly(*p*-phenylene) polymer was about $600 \text{ cm}^2 \text{ V}^{-1} \text{ s}^{-1}$.¹⁷ Therefore, reducing the torsional angles or using shape-persistent backbones might improve the effective conjugation length and thereby increase the intrachain transport. Furthermore, because the intrachain transport is much faster than interchain one, polymers with higher molecular weight usually display higher mobilities.^{4,18,19}

In conjugated polymer films, there are generally crystallized and amorphous zones, as indicated by the atomic force microscopy (AFM) image in Figure 1b. Thus, interchain transport is generally classified into two pathways: (i) transport at ordered packing zones, which may adopt a hopping mechanism like orderly packed small molecules (pathway 2 in Figure 1a); (ii) transport at loosely contacted zones, where carrier transport is slow (pathway 3 in Figure 1a). Clearly, ordered molecular packing effectively reduces the loosely contacted zones, thereby improving interchain transport. For pathway 2, charge transport is similar to the hopping process in small molecules, which is determined by two important factors: reorganization energy and electronic couplings.²⁰ Therefore, conjugated polymers with low reorganization energy and strong interchain electronic coupling are expected.

■ AMBIENT-STABLE FETS AND SIDE-CHAIN IMPEDIMENTS TO π - π STACKING

Since the first report of polythiophene FETs in 1986, electron-rich thiophene-based polymers have become one of the most extensively investigated classes.¹ Although several thiophene-based polymers provide mobilities over $0.5 \text{ cm}^2 \text{ V}^{-1} \text{ s}^{-1}$ and on/off ratios over 10^6 ,²¹ their stability is insufficient for practical applications.²² Thus, isoindigo was introduced to lower the HOMO levels of polythiophenes, ultimately improving the device stability.¹¹

The alkyl chain effect was also taken into account when designing the isoindigo-based polymers. Figure 2a shows the single crystal packing of *n*-hexane.²³ The shortest C–C distance (3.623 Å) comes from the methyl C atoms of adjacent columns, and the shortest distance between parallel packed alkyl chains is 4.065 Å. These distances are obviously larger than the π - π stacking distances (3.3–3.6 Å) found in many organic semiconductors.¹ Hence, a steric hindrance may impede the interchain π - π stacking of polymer backbones (Figure 2b). To avoid such hindrance, we proposed a “molecular docking” strategy by moving the alkyl chains from small (red cube) to the large (blue cube) units (Figure 2c). This strategy effectively reduces the steric hindrance caused by alkyl chains, thereby making the small aromatics “dock into” the large ones. In addition, large cores also reduce the reorganization energy when carrier hopping,²⁰ which was also used in the design of high-mobility small molecules.²⁴

On the basis of these considerations, we developed two isoindigo-based polymers, IIDDT and IIDT (Figure 2d).¹¹ 2-Octyldodecyl chains were used to guarantee good solubility. Molecular weights of both polymers were initially evaluated by gel permeation chromatography (GPC) using THF as eluent at room temperature. IIDT showed M_n of 19.8 kDa, whereas IIDDT showed high M_n of 87.9 kDa. However, when 1,2,4-trichlorobenzene (TCB) was used as eluent at 150 °C, M_n of IIDDT noticeably decreased to 33.7 kDa and that of IIDT remained at about 19.6 kDa. This result indicates that IIDDT had much stronger interchain interactions than IIDT. Cyclic voltammetry (CV) measurement showed that IIDDT had HOMO and LUMO levels of -5.65 and -3.78 eV, and IIDT had HOMO and LUMO levels of -5.80 and -3.81 eV. Both polymers showed clearly deeper HOMO levels compared with traditional thiophene-based polymers.

Bottom-gate/top-contact device configuration was used to fabricate the FET devices of both polymers. IIDT showed hole mobilities of only 0.01 – $0.02 \text{ cm}^2 \text{ V}^{-1} \text{ s}^{-1}$ after annealing at 150 °C. For IIDDT, the pristine films exhibited hole mobilities of

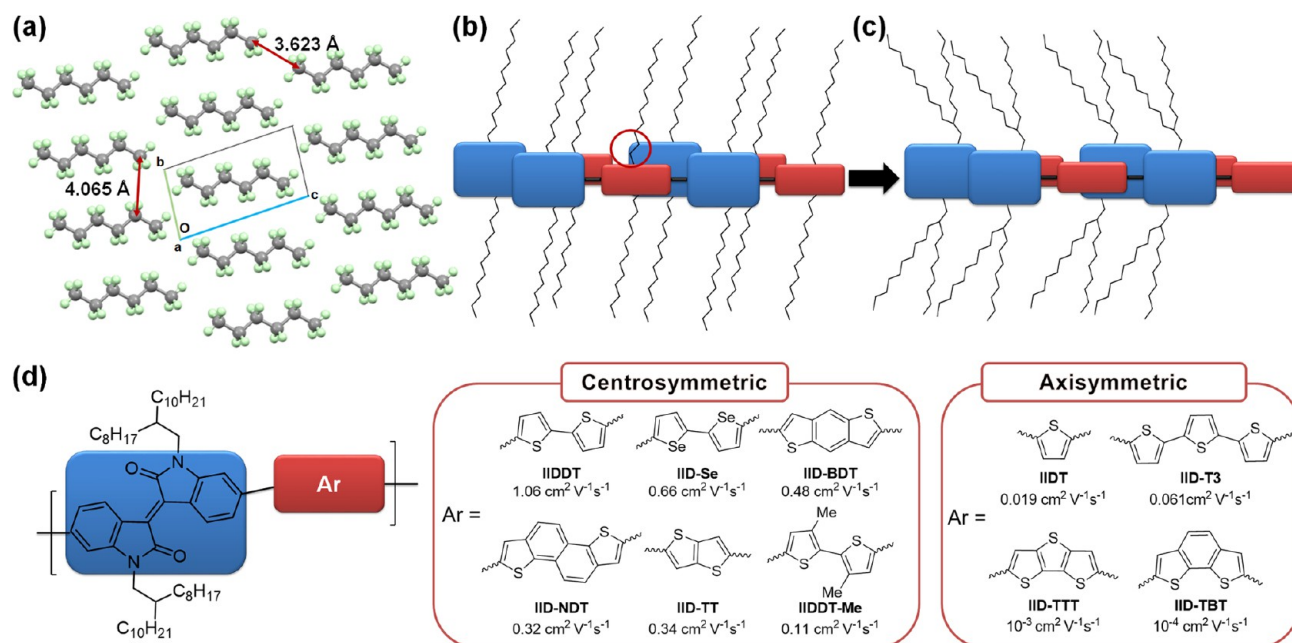


Figure 2. (a) Crystal packing of *n*-hexane viewed from the *a* axis.²³ (b) Polymers contain alkyl chains on both the donor and the acceptor. Steric hindrance may exist when polymers are stacked (red circle). (c) Proposed docking model to avoid the side-chain impediments after moving the alkyl chains from small (red cube) to the large cores (blue cube). (d) Chemical structures of isoindigo-based polymers with centrosymmetric and axisymmetric donors and their hole mobilities.

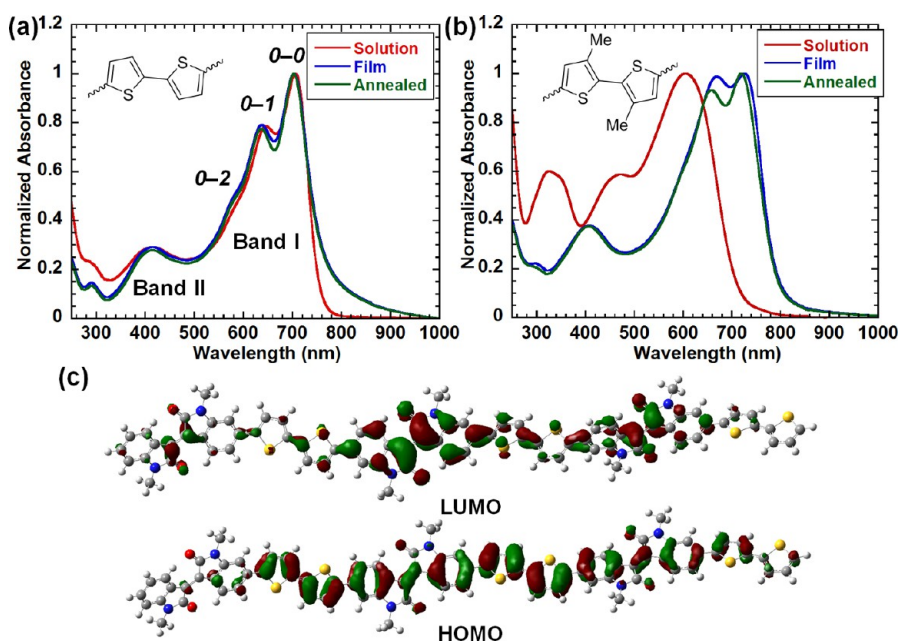


Figure 3. Normalized UV-vis absorption spectra of (a) IIDD and (b) IIDDT-Me in CHCl_3 ($1 \times 10^{-5} \text{ M}$), in film, and in annealed film and (c) molecular frontier orbitals of IIDDT trimer.

$0.1\text{--}0.2 \text{ cm}^2 \text{V}^{-1} \text{s}^{-1}$. After annealing at $150 \text{ }^\circ\text{C}$, IIDDT exhibited the highest hole mobility up to $0.79 \text{ cm}^2 \text{V}^{-1} \text{s}^{-1}$ and an average mobility of $0.42 \text{ cm}^2 \text{V}^{-1} \text{s}^{-1}$. When TCB was used, the maximum mobility of IIDDT further increased to $1.06 \text{ cm}^2 \text{V}^{-1} \text{s}^{-1}$ with an average mobility of $0.66 \text{ cm}^2 \text{V}^{-1} \text{s}^{-1}$.²⁵ More importantly, the devices of IIDDT showed excellent stability for 6 months under ambient conditions attributed to its low-lying HOMO level.

EFFECT OF DONOR SYMMETRY AND BACKBONE CURVATURE

Encouraged by the aforementioned results, we synthesized eight other isoindigo-based polymers to investigate the structure–property relationship.²⁵ These polymers were categorized to two groups according to the donor symmetries (Figure 2e). In order to prove the proposed “molecular docking” strategy, IIDDT-Me was also synthesized to compare it with IIDDT. We envisioned that the methyl groups may hinder the interchain $\pi\text{--}\pi$ stacking.

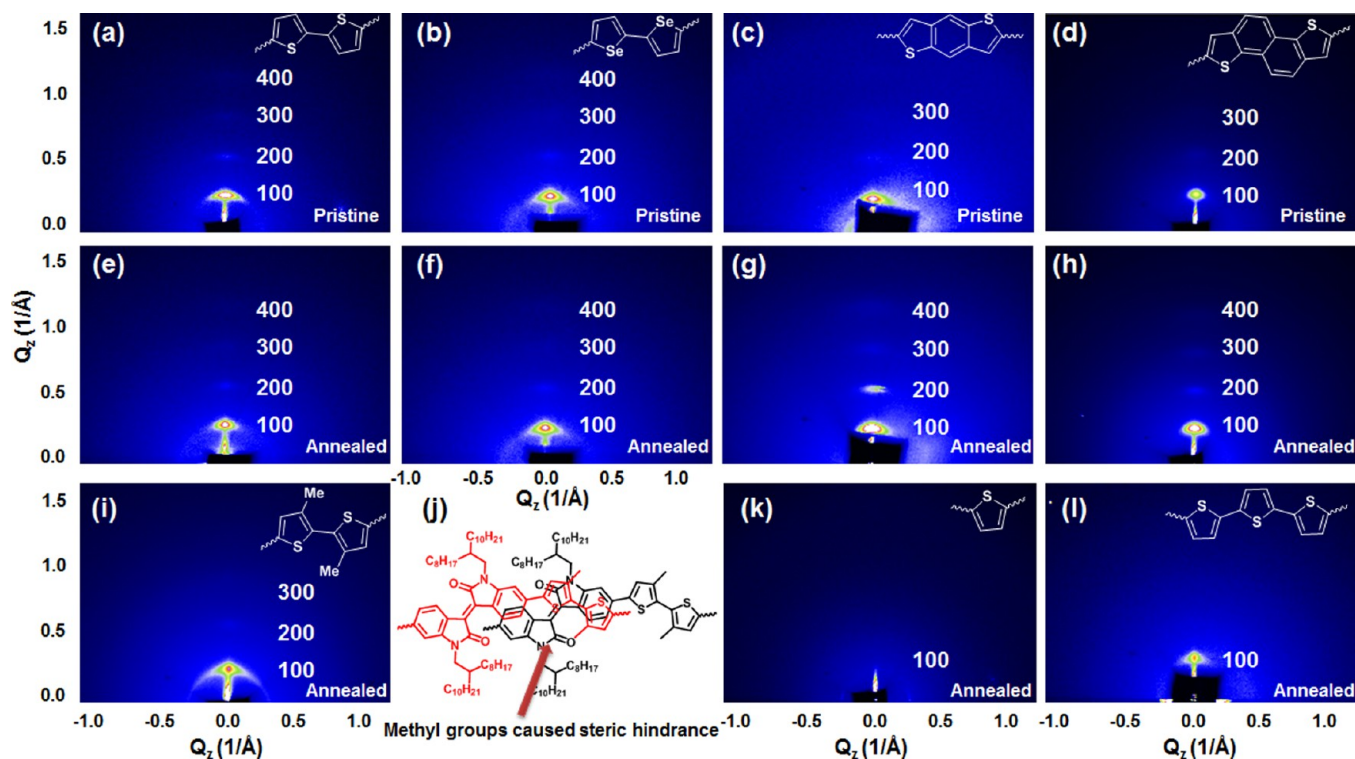


Figure 4. Two-dimensional GIXD patterns of (a, e) IIDDT, (b, f) IID-Se, (c, g) IID-BDT, (d, h) IID-NDT, (i) IIDDT-Me, (k) IIDT, and (l) IID-TTT pristine or annealed films. (j) Schematic representation of the steric hindrance caused by the methyl groups in IIDDT-Me.

These polymers generally have two absorption bands both in solution and in film: band I (500–800 nm) and band II (300–500 nm) (Figure 3a). Varying with different polymers, band II is attributed to the absorption of the donor part. However, these polymers have similar features in band I with three vibrational peaks, 0–0, 0–1, and 0–2, attributed to the charge-transfer absorption from the donor to the isoindigo core. Scrutiny of the spectra reveals that the 0–0 vibrational transition increased whereas 0–1 decreased when polymers were going from solution to film. After annealing, a further intensity increase of the 0–0 vibrational peak was observed, suggesting a further adjustment of polymer conformation. Methyl groups of IIDDT-Me resulted in great torsion angles in polymer backbone and broke the conjugation of the polymer in solution, thus leading to an obvious blue-shift. This torsion angle was suppressed in the solid state due to π – π stacking, significantly red-shifting the absorption spectrum (Figure 3b).

CV measurement of these polymers showed similar reductive potentials with LUMO levels around -3.70 eV. However, HOMO levels of the polymers varied with the electron-donating properties of the donor units. For example, when more electron-rich 2,2'-biselenophene unit was used, the HOMO level of IID-Se increased to -5.56 eV, whereas after introduction of less electron-rich donor benzodithiophene (BDT), the HOMO level of IID-BDT lowered to -5.84 eV. These results are consistent with the calculation that their LUMOs are mostly localized on the isoindigo core and the HOMOs are distributed along the polymer backbones (Figure 3c). Thus, the HOMO levels are more easily affected by the electronic structure of the donor, whereas the LUMO levels remain almost unchanged.

Except for IIDDT-Me, the other five polymers with centrosymmetric donors all showed hole mobilities over $0.3 \text{ cm}^2 \text{ V}^{-1} \text{ s}^{-1}$ (Figure 2e). IIDDT-Me showed the worst

performance with the maximum mobility of $0.11 \text{ cm}^2 \text{ V}^{-1} \text{ s}^{-1}$, almost 1 order of magnitude lower than that of IIDDT. We proposed that the methyl groups might hinder the interchain π – π stacking and thereby reduce the mobility. In sharp contrast, all polymers with axisymmetric donors exhibited much lower hole mobilities (Figure 2).

Grazing incident X-ray diffraction (GIXD) was employed to investigate the polymer packing in films (Figure 4). IIDDT, IID-Se, IID-BDT, and IID-NDT showed four out-of-plane diffraction peaks. After annealing, the intensity of diffraction peaks increased, suggesting that they formed better edge-on lamellar packing in the films. For IIDDT-Me, only three diffraction peaks were observed, and the 100 diffraction was broader compared with that of IIDDT, indicating a relatively disordered lamellar packing. Presumably the methyl groups in IIDDT-Me hindered the interchain π – π stacking, which further deteriorated the out-of-plane packing. In contrast, all polymers containing axisymmetric donors showed poor lamellar packing. IIDT and IID-T3 displayed only one diffraction peak with larger lamellar packing distance. For IID-TTT and IID-TBT, no obvious diffraction peak was observed. AFM images also showed that polymers with centrosymmetric units exhibited obviously larger crystallized zones and fibrillar intercalating networks with high surface roughness in films. In contrast, polymers with axisymmetric units showed smooth and amorphous films.

These results indicate that the device performances may correlate with the film morphologies and interchain packing of the polymers. Polymers with centrosymmetric units exhibited better crystallinity and lamellar packing in film due to the good interchain π – π stacking. As shown in Figure 5a, for those polymers with centrosymmetric donors, the “small units” readily dock into the cavity formed by the “large core” and branched alkyl chains. The interchain D–A interaction further

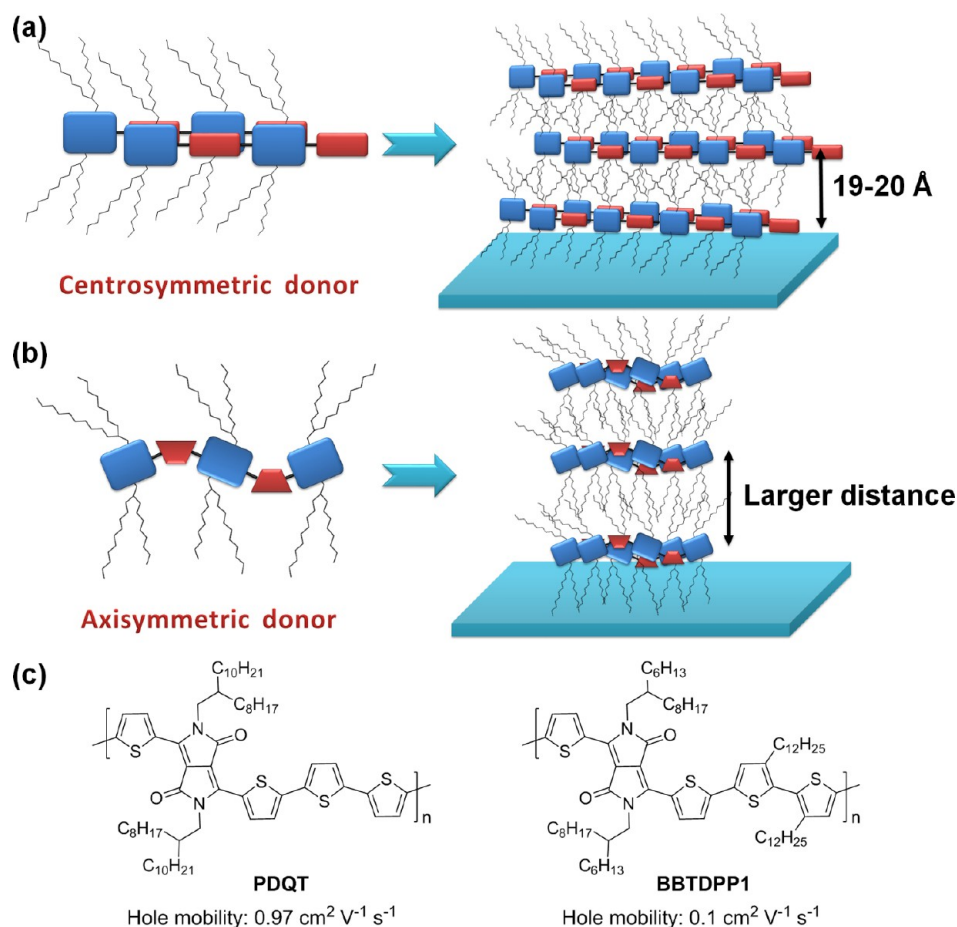


Figure 5. Schematic representation of isoidigo-based polymers with different symmetries and their film packing (a) with centrosymmetric and (b) with axisymmetric donors and (c) impediment of side chains observed in DPP-based polymers.^{28,29}

enhanced the docking. In addition, these polymer backbones are almost linear and parallel to the substrate. Their decent π - π stacking and the linear backbone lead to good lamellar packing in the film. With a linear backbone, IIDDT-Me also showed good lamellar packing yet poor mobility, presumably due to the poor π - π stacking. Polymer backbones containing axisymmetric donors, nonetheless, became zigzag, inhibiting the “molecular docking” and lamellar packing in the film (Figure 5b). With the most linear backbone, IID-T3 showed the best hole mobility up to $0.061 \text{ cm}^2 \text{ V}^{-1} \text{ s}^{-1}$, indicating the importance of backbone curvature. The important effects of building block symmetry and backbone curvature on polymer FETs were also observed in other polymer systems.^{26,27} In addition, the strategy to avoid the impediment of alkyl chains is also applicable to DPP-based polymers. With an identical backbone to PDQT²⁸ but two additional dodecyl chains, BBTDPPI showed hole mobility as high as $0.1 \text{ cm}^2 \text{ V}^{-1} \text{ s}^{-1}$,²⁹ almost 1 order of magnitude lower than PDQT (Figure 5c).

■ INFLUENCE OF THE BRANCHING POSITION OF SIDE CHAINS

Side chains in conjugated polymers are more than just solubilizing groups. They play important roles in physical properties and molecular packing and hence device performance.^{30–32} Compared with linear ones, branched alkyl chains generally provide better solubility. Interestingly, the distance of the branching point of these chains to the conjugated backbone is only one methylene group. As discussed above, alkyl chains

may impede interchain π - π interactions. Similarly, when the branching points are close to polymer backbones, steric hindrance may also occur due to the large van der Waals radii in the branching position (Figure 6a). To increase the structural diversity of solubilizing groups, Bao designed an unconventional siloxane-terminated chain (Figure 6b),³³ which exhibited closer backbone packing and increased hole mobility up to $2.48 \text{ cm}^2 \text{ V}^{-1} \text{ s}^{-1}$. However, the trimethylsilyl group cannot survive under certain reaction conditions, limiting its application. Thus, we designed three novel branched alkyl chains (3-decyltridecyl, 4-decyltetradecyl, and 5-decylpentadecyl) to modify the polymer (Figure 6c). We investigated how moving the branching point of these “more convectional” alkyl chains farther from the backbone influences the mobilities.¹⁵

Although the corresponding monomers with different alkyl chains showed almost identical photophysical and electrochemical properties, these polymers exhibited distinctly different properties. Compared with IIDDT and IIDDT-C2, IIDDT-C3 and IIDDT-C4 showed red-shifted absorption both in solution and in the solid state (Figure 7a). The main absorption peaks of these polymers in films only showed a very little red-shift compared with those in solution. The absence of the bathochromic effects indicated that the polymers probably formed some preaggregates in solution.³⁴ Farther branched alkyl chains reduce the steric hindrance effects of interchain interaction, thus leading to a closer π - π stacking distance. Shorter π - π stacking distance suppresses the polymer backbone twisting and make the backbone more planar,

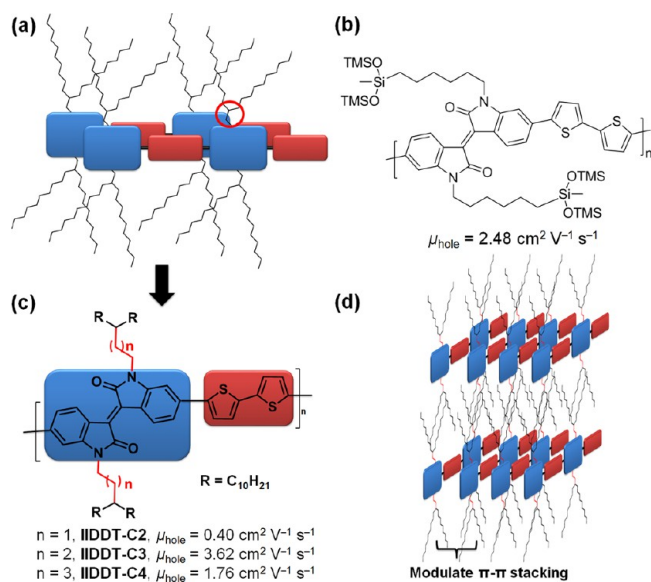


Figure 6. (a) Schematic representation of the impediment of branching position of alkyl chains (red circle). (b) Polymers with siloxane-terminated side chains.³³ (c) Sequentially variation of the branching position of the alkyl chains of IIDDT. (d) A proposed packing model of the polymers in the film.

thereby resulting in the bathochromic phenomena of IIDDT-C3 and IIDDT-C4. Moving the branching point away from the polymer backbones also led to a noticeable increase of the HOMO levels from -5.70 (IIDDT) to -5.50 eV (IIDDT-C4). But the LUMO levels showed only slight decrease from -3.70 (IIDDT) to -3.74 eV (IIDDT-C4). This result may be again due to the closer π - π stacking and backbone planarization of IIDDT-C3 and IIDDT-C4.

IIDDT-C3 exhibited a high hole mobility up to $3.62 \text{ cm}^2 \text{ V}^{-1} \text{ s}^{-1}$ after annealing, significantly higher than that of IIDDT. IIDDT-C4 displayed increased mobility up to $1.76 \text{ cm}^2 \text{ V}^{-1} \text{ s}^{-1}$. Unexpectedly, IIDDT-C2 showed decreased device performance with the highest mobility only $0.40 \text{ cm}^2 \text{ V}^{-1} \text{ s}^{-1}$. To gain further understanding, GIXD experiments demonstrated that all four polymers displayed a long-range ordered edge-on lamellar packing, and the measured lamellar distance increased with the increase of alkyl chain lengths (Figure 7b–d). In in-plane diffractions, the polymers showed gradually decreased

π - π stacking distances (3.75 \AA for IIDDT, 3.61 \AA for IIDDT-C2, and 3.57 \AA for both IIDDT-C3 and IIDDT-C4) after the branching point was moved away from the backbone. Thus, the significantly improved mobilities are largely due to the decreased π - π stacking distances. However, the mobilities of the polymers did not always increase with the decrease of the π - π stacking distances. Such inconsistency between device performances and π - π stacking distances is probably caused by the different stacking conformations of the polymers, which also plays a vital role in interchain carrier transport.

■ CORE ENGINEERING TO ACHIEVE AMBIPOLAR TRANSPORT AND IMPROVE DEVICE STABILITY

Isoidingo-based polymers exhibited extremely low electron mobilities (the highest one is only $3.7 \times 10^{-7} \text{ cm}^2 \text{ V}^{-1} \text{ s}^{-1}$),³⁵ thus limiting their applications in organic electronics. An effective approach to increase and stabilize electron transport is to lower polymer LUMO levels. The aforementioned results have shown that changing the donor part can hardly affect the LUMO levels of isoidingo-based polymers. Thus, we focused on engineering the isoidingo core, and both fluorine and chlorine were introduced (Figure 8).^{36,37} Fluorine is capable of modulating the electronic properties of polymers without deleterious steric effects. Although chlorine has been demonstrated to be an effective functional group for lowering the LUMO levels, chlorination on conjugated polymers was not reported, presumably due to its larger atom size and thereby stronger steric hindrance effect.³⁸

Figure 8 shows the computational analysis of the fragment structures of three polymers. The introduction of fluorine atoms does not increase the dihedral angle of polymer backbones. Instead, because of fluorine–hydrogen interaction, the phenyl–thienyl rotational angle decreases from 22.2° to 17.1° , and the calculated F–H distance (2.27 \AA) is significantly shorter than the sum of the F–H van der Waals radii (2.56 \AA). Although a Cl–H interaction also exists in PCII2T, the dihedral angle still increases to 34.2° due to the large size of chlorine atoms. Such difference of the dihedral angle was also reflected in their absorption features. Smaller dihedral angles led to stronger 0–0 and weaker 0–1 vibrational absorptions, and vice versa. Note that core engineering of isoidingo effectively lowers the LUMO levels, whereas changing the donor of isoidingo-based polymers hardly affects the LUMO levels. Both the

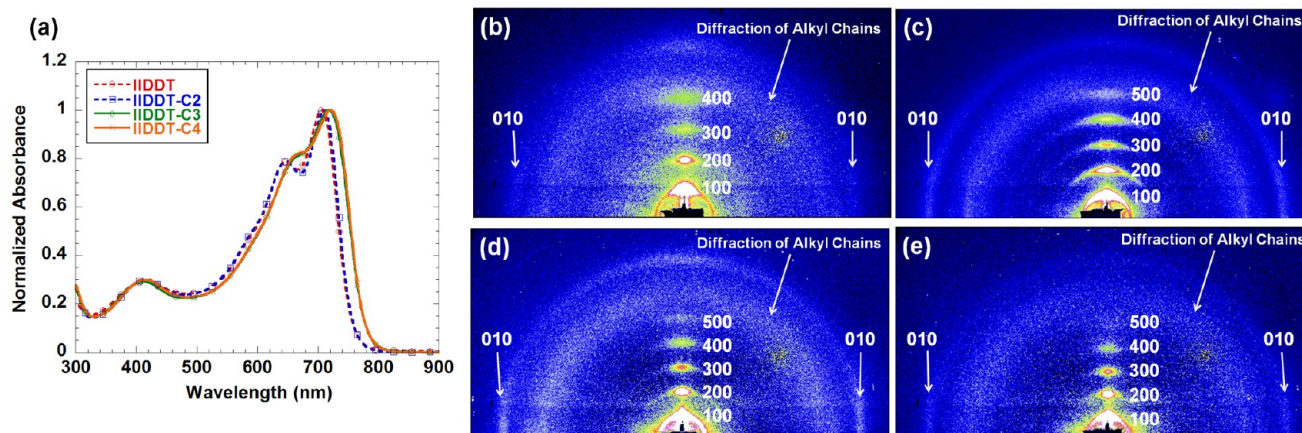


Figure 7. (a) Normalized UV-vis absorption spectra of four polymers in CHCl_3 ($1 \times 10^{-5} \text{ M}$) and two-dimensional GIXD patterns of (b) IIDDT, (c) IIDDT-C2, (d) IIDDT-C3, and (e) IIDDT-C4 films after annealing.

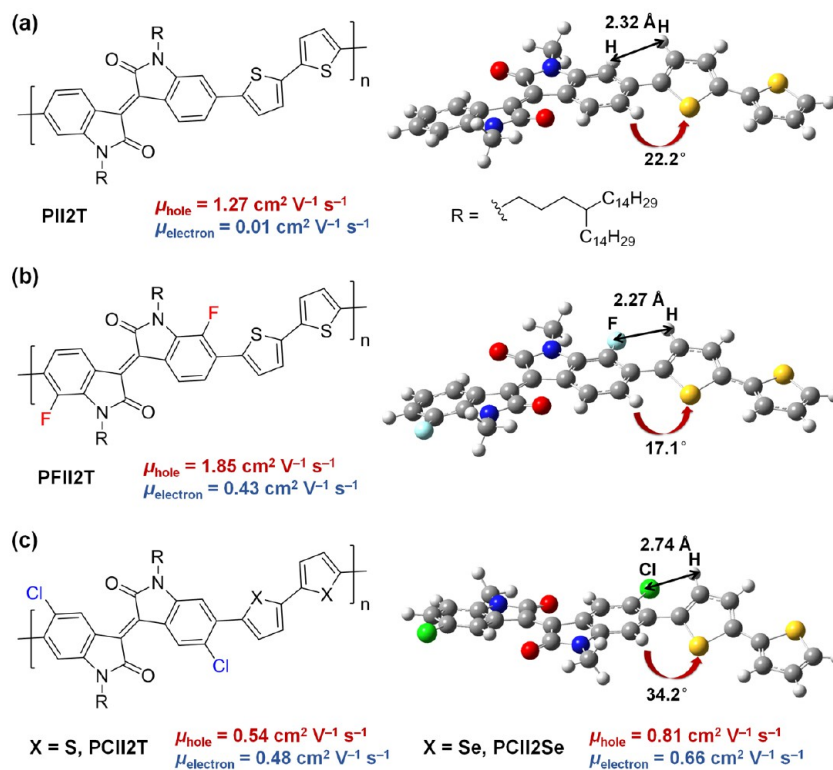


Figure 8. Chemical structures, molecular models, and FET mobilities of (a) PII2T, (b) PFII2T, and (c) PCII2T and PCII2Se. All FET mobilities are obtained from the devices fabricated under ambient conditions.

HOMO and LUMO levels of PFII2T (-5.60 and -3.88 eV) and PCII2T (-5.64 and -3.86 eV) through the introduction of both fluorine and chlorine are lower than those of PII2T (-5.42 and -3.70 eV).

Top-gate/bottom-contact devices were fabricated using these polymers both in a glovebox and in ambient conditions ($R_H = 50\text{--}60\%$). PII2T showed high hole mobility up to $0.76\text{ cm}^2\text{ V}^{-1}\text{ s}^{-1}$ and low electron mobility of $0.07\text{ cm}^2\text{ V}^{-1}\text{ s}^{-1}$; after exposure to air, the hole mobility increased to $1.27\text{ cm}^2\text{ V}^{-1}\text{ s}^{-1}$ but the electron mobility decreased drastically to $10^{-3}\text{--}10^{-2}\text{ cm}^2\text{ V}^{-1}\text{ s}^{-1}$. In contrast, PFII2T devices fabricated under ambient conditions showed remarkably high hole mobility up to $1.85\text{ cm}^2\text{ V}^{-1}\text{ s}^{-1}$ and obviously increased electron mobility up to $0.43\text{ cm}^2\text{ V}^{-1}\text{ s}^{-1}$, slightly lower than those fabricated in a glovebox ($0.51\text{ cm}^2\text{ V}^{-1}\text{ s}^{-1}$). PCII2T showed balanced hole and electron transports. For devices fabricated in a glovebox, hole mobility up to $0.50\text{ cm}^2\text{ V}^{-1}\text{ s}^{-1}$ and electron mobility up to $0.62\text{ cm}^2\text{ V}^{-1}\text{ s}^{-1}$ were observed; for those fabricated under ambient conditions, the hole mobility slightly increased to $0.54\text{ cm}^2\text{ V}^{-1}\text{ s}^{-1}$ and the electron mobility slightly decreased to $0.48\text{ cm}^2\text{ V}^{-1}\text{ s}^{-1}$. Besides the 2,2'-bithiophene one, a 2,2'-biselenophene unit was also used. With PCII2Se, high hole and electron mobilities up to 1.05 and $0.72\text{ cm}^2\text{ V}^{-1}\text{ s}^{-1}$, respectively, were obtained for devices fabricated in a glovebox, and the hole mobility ($0.81\text{ cm}^2\text{ V}^{-1}\text{ s}^{-1}$) and electron mobility ($0.66\text{ cm}^2\text{ V}^{-1}\text{ s}^{-1}$) only decreased slightly under ambient conditions. Hence, the introduction of fluorine and chlorine atoms improved both the electron mobility and the ambient stability of isoindigo polymers. Complementary-like inverters based on chlorinated polymers were also demonstrated, exhibiting a sharp signal switching with high gains up to 48 due to their balanced carrier transport. Furthermore, GIXD investigation showed that the introduction of fluorine and

chlorine atoms and selenophene not only modulated the energy levels but also affected the interchain interactions and led to different polymer packing in the solid state. Figure 9 shows that PII2T preferred to form face-on packing in film; however, both edge-on and face-on packing were found in PCII2T, and no face-on packing was observed in PCII2Se. Very recently, fluorinated isoindigo polymers were also used for solar cells to enhance the open circuit voltage and power conversion efficiency,^{12,39} thus demonstrating the broad applications of core functionalized isoindigo derivatives.

■ CORE EXTENSION TO BUILD UP NEW SYSTEMS

To further modulate the electronic properties of isoindigo, we designed three novel structures based on isoindigo by breaking the double bond between two lactam rings and inserting different π -conjugated skeletons (Figure 10a). Only the third structure (BDOPV) was successfully obtained, probably due to four intermolecular hydrogen bonds that provide extra stability.⁴⁰ BDOPV is a novel derivative of oligo(*p*-phenylenevinylene) (OPV) but exhibits a low LUMO of -4.24 eV. Through polymerization with (*E*)-1,2-bis(tributylstannyl)ethene, an electron-deficient poly(*p*-phenylenevinylene) (PPV) derivative (BDPPV) was obtained. This new PPV derivative displayed high electron mobilities up to $1.1\text{ cm}^2\text{ V}^{-1}\text{ s}^{-1}$ under ambient conditions (4 orders of magnitude higher than those of other PPVs), because it overcame common defects in PPVs, such as conformational disorder, weak interchain interaction, and high LUMO level.

A powerful strategy to achieve high carrier mobility is the synthesis of an alternating conjugated polymer from electron-rich and electron-deficient units.⁷ BDOPV was used to construct a D–A polymer BDOPV-2T (Figure 9c),⁴¹ which

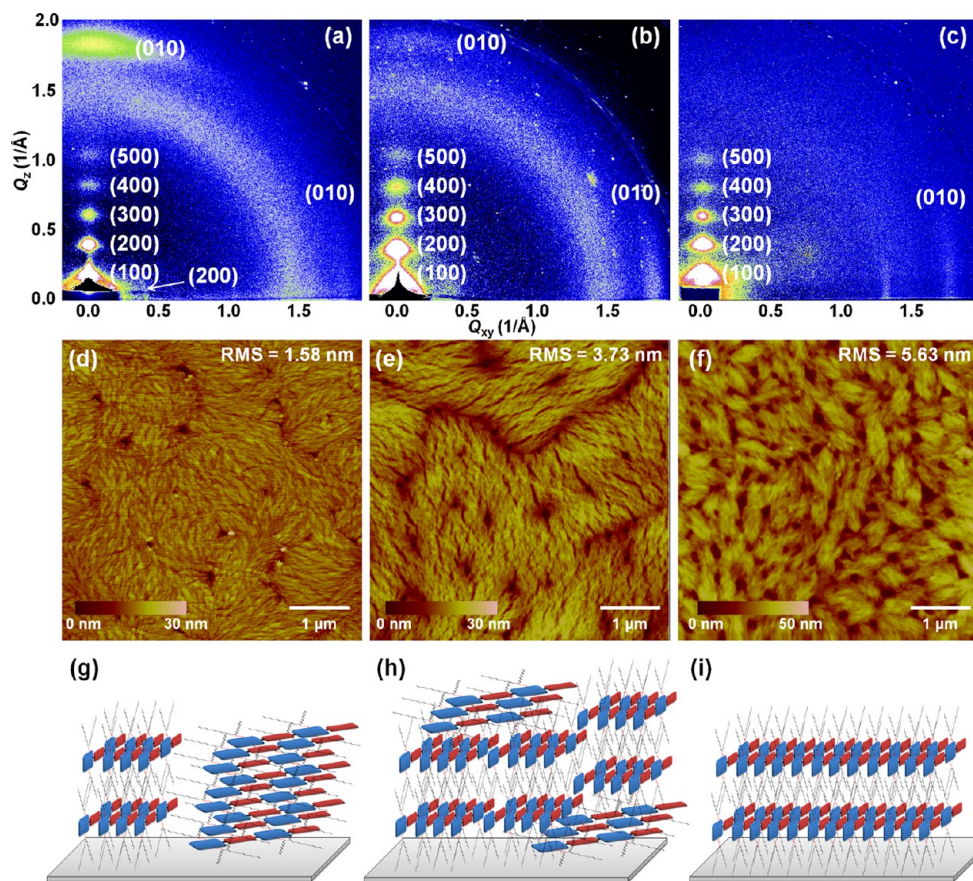


Figure 9. Two-dimensional GIXD patterns, AFM height images, and cartoon illustration of the proposed packing models of (a, d, g) PII2T, (b, e, h) PCI2T, and (c, f, i) PCI2Se films.

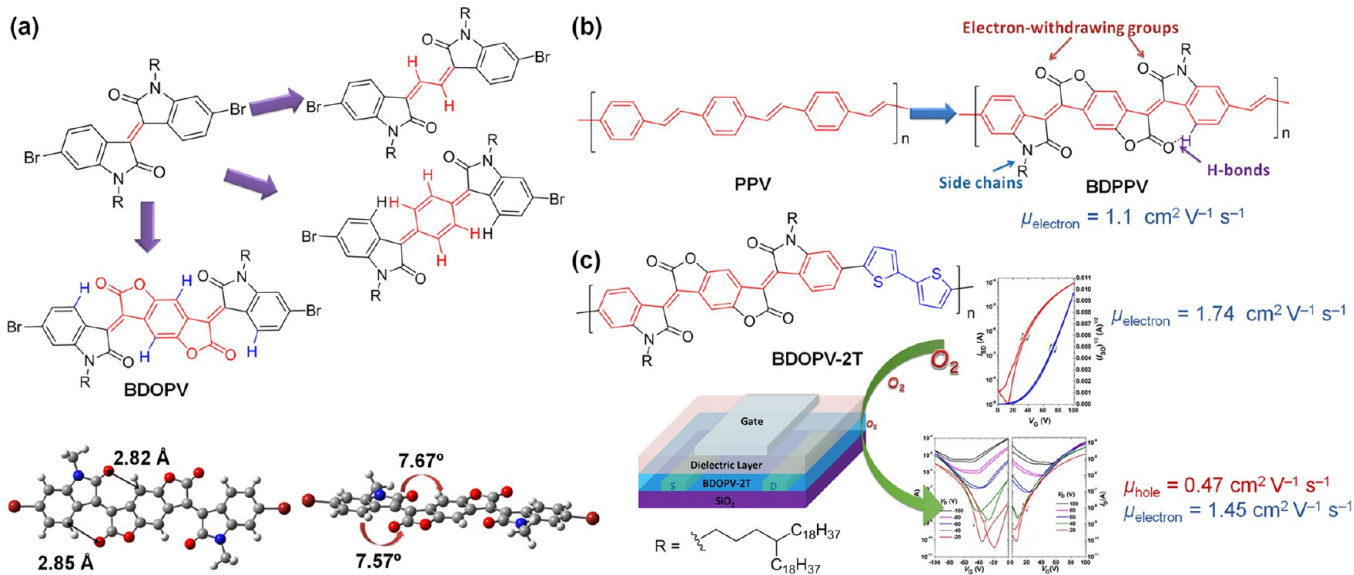


Figure 10. (a) Proposed core extension strategy for isoindigo. (b) Electron-deficient BDPPV was constructed. (c) BDOPV-2T for n-type and oxygen-doped ambipolar FETs.

showed a high electron mobility of $1.74 \text{ cm}^2 \text{ V}^{-1} \text{ s}^{-1}$. Upon oxygen exposure, BDOPV-2T displayed interesting ambipolar transporting behavior, while maintaining high electron mobilities up to $1.45 \text{ cm}^2 \text{ V}^{-1} \text{ s}^{-1}$, along with significantly increased hole mobilities up to $0.47 \text{ cm}^2 \text{ V}^{-1} \text{ s}^{-1}$. Li et al. independently synthesized two structurally similar BDOPV-

based polymers. Nonetheless, one polymer was insoluble, and another only showed hole and electron mobilities around $0.01 \text{ cm}^2 \text{ V}^{-1} \text{ s}^{-1}$.⁴² This is probably caused by the axisymmetric donors and the close branching position of the side chains, thereby further demonstrating that the synergy of polymer

backbone and side chain engineering is essential to achieve high performance in conjugated polymers.

SUMMARY AND OUTLOOK

From the design of high-stability p-type FETs to the realization of ambient-stable ambipolar FETs, from the consideration of the impediment of alkyl chains to the variation of the branching position of side chains, and from the engineering of donor symmetry to the extension of the isoindigo unit, we outline recent progress and several design strategies in isoindigo-based polymers. A synergy of the molecular engineering strategies toward the isoindigo core, donor units, and side chains not only improves the device performance and broadens the application of isoindigo polymers but also enables a better fundamental understanding of the structure–property relationships in conjugated polymers. Many results demonstrate that these developments and design strategies are also significant for other polymer systems and even small molecules.^{3,30,43–45} However, to advance the practical application of isoindigo-based polymers, some challenges persist, especially in further enhancing both hole and electron mobilities, better controlling the molecular packing, and substantially improving the device reproducibility and stability, which call for the integrated consideration of both molecular design and process engineering and the collective efforts of scientists in multiple disciplines.

AUTHOR INFORMATION

Corresponding Author

*E-mail: jianpei@pku.edu.cn.

Notes

The authors declare no competing financial interest.

Biographies

Ting Lei received his B.Sc. degree from Peking University in 2008. He continued his study in the Pei group and obtained his Ph.D. degree in 2013. His interests include the synthesis, characterization and mechanistic investigation of organic materials.

Jie-Yu Wang is currently an Assistant Professor in Peking University. She received her Ph.D. degree from Peking University in 2009. Her interests relate to organic synthesis, supramolecular chemistry, and fabrication of organic materials.

Jian Pei received his B.Sc. and Ph.D. degrees from Peking University. In 1998, he joined the group of Professor Alan J. Heeger to study organic semiconducting materials. He came back to Peking University in 2001. His interests relate to organic synthesis, supramolecular chemistry, organic semiconductors and optoelectronic devices.

ACKNOWLEDGMENTS

This work was supported by the Major State Basic Research Development Program (2013CB933500), and by the National Natural Science Foundation of China.

REFERENCES

- (1) Wang, C.; Dong, H.; Hu, W.; Liu, Y.; Zhu, D. Semiconducting π -Conjugated Systems in Field-Effect Transistors: A Material Odyssey of Organic Electronics. *Chem. Rev.* **2012**, *112*, 2208–2267.
- (2) Beaujuge, P. M.; Fréchet, J. M. J. Molecular Design and Ordering Effects in π -Functional Materials for Transistor and Solar Cell Applications. *J. Am. Chem. Soc.* **2011**, *133*, 20009–20029.
- (3) Mei, J.; Diao, Y.; Appleton, A. L.; Fang, L.; Bao, Z. Integrated Materials Design of Organic Semiconductors for Field-Effect Transistors. *J. Am. Chem. Soc.* **2013**, *135*, 6724–6746.

- (4) Li, J.; Zhao, Y.; Tan, H. S.; Guo, Y.; Di, C.-A.; Yu, G.; Liu, Y.; Lin, M.; Lim, S. H.; Zhou, Y.; Su, H.; Ong, B. S. A Stable Solution-Processed Polymer Semiconductor with Record High-Mobility for Printed Transistors. *Sci. Rep.* **2012**, *2*, 754.

- (5) Kanimozhi, C.; Yaacobi-Gross, N.; Chou, K. W.; Amassian, A.; Anthopoulos, T. D.; Patil, S. Diketopyrrolopyrrole-Diketopyrrolopyrrole-Based Conjugated Copolymer for High-Mobility Organic Field-Effect Transistors. *J. Am. Chem. Soc.* **2012**, *134*, 16532–16535.

- (6) Heeger, A. J. Semiconducting Polymers: The Third Generation. *Chem. Soc. Rev.* **2010**, *39*, 2354–2371.

- (7) Yuen, J. D.; Wudl, F. Strong Acceptors in Donor-Acceptor Polymers for High Performance Thin Film Transistors. *Energy Environ. Sci.* **2013**, *6*, 392–406.

- (8) Nielsen, C. B.; Turbiez, M.; McCulloch, I. Recent Advances in the Development of Semiconducting DPP-Containing Polymers for Transistor Applications. *Adv. Mater.* **2013**, *25*, 1859–1880.

- (9) Zhan, X.; Facchetti, A.; Barlow, S.; Marks, T. J.; Ratner, M. A.; Wasielewski, M. R.; Marder, S. R. Rylene and Related Diimides for Organic Electronics. *Adv. Mater.* **2011**, *23*, 268–284.

- (10) Mei, J.; Graham, K. R.; Stalder, R.; Reynolds, J. R. Synthesis of Isoindigo-Based Oligothiophenes for Molecular Bulk Heterojunction Solar Cells. *Org. Lett.* **2010**, *12*, 660–663.

- (11) Lei, T.; Cao, Y.; Fan, Y.; Liu, C.-J.; Yuan, S.-C.; Pei, J. High-Performance Air-Stable Organic Field-Effect Transistors: Isoindigo-Based Conjugated Polymers. *J. Am. Chem. Soc.* **2011**, *133*, 6099–6101.

- (12) Deng, Y.; Liu, J.; Wang, J.; Liu, L.; Li, W.; Tian, H.; Zhang, X.; Xie, Z.; Geng, Y.; Wang, F. Dithienocarbazole and Isoindigo Based Amorphous Low Bandgap Conjugated Polymers for Efficient Polymer Solar Cells. *Adv. Mater.* **2014**, *26*, 471–476.

- (13) Kim, D. H.; Ayzner, A. L.; Appleton, A. L.; Schmidt, K.; Mei, J.; Toney, M. F.; Bao, Z. Comparison of the Photovoltaic Characteristics and Nanostructure of Fullerenes Blended with Conjugated Polymers with Siloxane-Terminated and Branched Aliphatic Side Chains. *Chem. Mater.* **2013**, *25*, 431–440.

- (14) Wang, E.; Ma, Z.; Zhang, Z.; Vandewal, K.; Henriksson, P.; Inganäs, O.; Zhang, F.; Andersson, M. R. An Easily Accessible Isoindigo-Based Polymer for High-Performance Polymer Solar Cells. *J. Am. Chem. Soc.* **2011**, *133*, 14244–14247.

- (15) Lei, T.; Dou, J.-H.; Pei, J. Influence of Alkyl Chain Branching Positions on the Hole Mobilities of Polymer Thin-Film Transistors. *Adv. Mater.* **2012**, *24*, 6457–6461.

- (16) Grozema, F. C.; van Duijnen, P. T.; Berlin, Y. A.; Ratner, M. A.; Siebbeles, L. D. A. Intramolecular Charge Transport along Isolated Chains of Conjugated Polymers: Effect of Torsional Disorder and Polymerization Defects. *J. Phys. Chem. B* **2002**, *106*, 7791–7795.

- (17) Prins, P.; Grozema, F. C.; Schins, J. M.; Patil, S.; Scherf, U.; Siebbeles, L. D. A. High Intrachain Hole Mobility on Molecular Wires of Ladder-Type Poly(*p*-Phenylenes). *Phys. Rev. Lett.* **2006**, *96*, No. 146601.

- (18) Tseng, H.-R.; Ying, L.; Hsu, B. B. Y.; Perez, L. A.; Takacs, C. J.; Bazan, G. C.; Heeger, A. J. High Mobility Field Effect Transistors Based on Macroscopically Oriented Regioregular Copolymers. *Nano Lett.* **2012**, *12*, 6353–6357.

- (19) Tsao, H. N.; Cho, D. M.; Park, I.; Hansen, M. R.; Mavrinskiy, A.; Yoon, D. Y.; Graf, R.; Pisula, W.; Spiess, H. W.; Müllen, K. Ultrahigh Mobility in Polymer Field-Effect Transistors by Design. *J. Am. Chem. Soc.* **2011**, *133*, 2605–2612.

- (20) Coropceanu, V.; Cornil, J.; da Silva Filho, D. A.; Olivier, Y.; Silbey, R.; Brédas, J.-L. Charge Transport in Organic Semiconductors. *Chem. Rev.* **2007**, *107*, 926–952.

- (21) McCulloch, I.; Heeney, M.; Bailey, C.; Genevicius, K.; MacDonald, I.; Shkunov, M.; Sparrowe, D.; Tierney, S.; Wagner, R.; Zhang, W.; Chabinyc, M. L.; Kline, R. J.; McGehee, M. D.; Toney, M. F. Liquid-Crystalline Semiconducting Polymers with High Charge-Carrier Mobility. *Nat. Mater.* **2006**, *5*, 328–333.

- (22) Osaka, I.; Takimiya, K.; McCullough, R. D. Benzobisthiazole-Based Semiconducting Copolymers Showing Excellent Environmental Stability in High-Humidity Air. *Adv. Mater.* **2010**, *22*, 4993–4997.

- (23) Boese, R.; Weiss, H.-C.; Bläser, D. The Melting Point Alternation in the Short-Chain *n*-Alkanes: Single-Crystal X-Ray Analyses of Propane at 30 K and of *n*-Butane to *n*-Nonane at 90 K. *Angew. Chem., Int. Ed.* **1999**, *38*, 988–992.
- (24) Takimiya, K.; Shinamura, S.; Osaka, I.; Miyazaki, E. Thienoacene-Based Organic Semiconductors. *Adv. Mater.* **2011**, *23*, 4347–4370.
- (25) Lei, T.; Cao, Y.; Zhou, X.; Peng, Y.; Bian, J.; Pei, J. Systematic Investigation of Isoindigo-Based Polymeric Field-Effect Transistors: Design Strategy and Impact of Polymer Symmetry and Backbone Curvature. *Chem. Mater.* **2012**, *24*, 1762–1770.
- (26) He, M.; Li, J.; Tandia, A.; Sorensen, M.; Zhang, F.; Fong, H. H.; Pozdin, V. A.; Smilgies, D.-M.; Malliaras, G. G. Importance of C_2 Symmetry for the Device Performance of a Newly Synthesized Family of Fused-Ring Thiophenes. *Chem. Mater.* **2010**, *22*, 2770–2779.
- (27) Osaka, I.; Abe, T.; Shinamura, S.; Takimiya, K. Impact of Isomeric Structures on Transistor Performances in Naphthodithiophene Semiconducting Polymers. *J. Am. Chem. Soc.* **2011**, *133*, 6852–6860.
- (28) Li, Y.; Sonar, P.; Singh, S. P.; Soh, M. S.; van Meurs, M.; Tan, J. Annealing-Free High-Mobility Diketopyrrolopyrrole–Quaterthiophene Copolymer for Solution-Processed Organic Thin Film Transistors. *J. Am. Chem. Soc.* **2011**, *133*, 2198–2204.
- (29) Bürgi, L.; Turbiez, M.; Pfeiffer, R.; Bienewald, F.; Kirner, H.-J.; Winnewisser, C. High-Mobility Ambipolar Near-Infrared Light-Emitting Polymer Field-Effect Transistors. *Adv. Mater.* **2008**, *20*, 2217–2224.
- (30) Lei, T.; Wang, J.-Y.; Pei, J. Roles of Flexible Chains in Organic Semiconducting Materials. *Chem. Mater.* **2014**, *26*, 594–603.
- (31) Mei, J.; Bao, Z. Side Chain Engineering in Solution-Processable Conjugated Polymers. *Chem. Mater.* **2014**, *26*, 604–615.
- (32) McCulloch, I.; Ashraf, R. S.; Biniek, L.; Bronstein, H.; Combe, C.; Donaghey, J. E.; James, D. L.; Nielsen, C. B.; Schroeder, B. C.; Zhang, W. Design of Semiconducting Indacenodithiophene Polymers for High Performance Transistors and Solar Cells. *Acc. Chem. Res.* **2012**, *45*, 714–722.
- (33) Mei, J.; Kim, D. H.; Ayzner, A. L.; Toney, M. F.; Bao, Z. Siloxane-Terminated Solubilizing Side Chains: Bringing Conjugated Polymer Backbones Closer and Boosting Hole Mobilities in Thin-Film Transistors. *J. Am. Chem. Soc.* **2011**, *133*, 20130–20133.
- (34) Zhou, N.; Guo, X.; Ortiz, R. P.; Li, S.; Zhang, S.; Chang, R. P. H.; Facchetti, A.; Marks, T. J. Bithiophene Imide and Benzodithiophene Copolymers for Efficient Inverted Polymer Solar Cells. *Adv. Mater.* **2012**, *24*, 2242–2248.
- (35) Stalder, R.; Mei, J.; Subbiah, J.; Grand, C.; Estrada, L. A.; So, F.; Reynolds, J. R. *n*-Type Conjugated Polyisoindigos. *Macromolecules* **2011**, *44*, 6303–6310.
- (36) Lei, T.; Dou, J.-H.; Ma, Z.-J.; Yao, C.-H.; Liu, C.-J.; Wang, J.-Y.; Pei, J. Ambipolar Polymer Field-Effect Transistors Based on Fluorinated Isoindigo: High Performance and Improved Ambient Stability. *J. Am. Chem. Soc.* **2012**, *134*, 20025–20028.
- (37) Lei, T.; Dou, J.-H.; Ma, Z.-J.; Liu, C.-J.; Wang, J.-Y.; Pei, J. Chlorination as a Useful Method to Modulate Conjugated Polymers: Balanced and Ambient-Stable Ambipolar High-Performance Field-Effect Transistors and Inverters Based on Chlorinated Isoindigo Polymers. *Chem. Sci.* **2013**, *4*, 2447–2452.
- (38) Tang, M. L.; Bao, Z. Halogenated Materials as Organic Semiconductors. *Chem. Mater.* **2011**, *23*, 446–455.
- (39) Yang, Y.; Wu, R.; Wang, X.; Xu, X.; Li, Z.; Li, K.; Peng, Q. Isoindigo Fluorination to Enhance Photovoltaic Performance of Donor-Acceptor Conjugated Copolymers. *Chem. Commun.* **2014**, *50*, 439–441.
- (40) Lei, T.; Dou, J.-H.; Cao, X.-Y.; Wang, J.-Y.; Pei, J. Electron-Deficient Poly(*p*-Phenylene Vinylene) Provides Electron Mobility over $1 \text{ cm}^2 \text{ V}^{-1} \text{ s}^{-1}$ under Ambient Conditions. *J. Am. Chem. Soc.* **2013**, *135*, 12168–12171.
- (41) Lei, T.; Dou, J.-H.; Cao, X.-Y.; Wang, J.-Y.; Pei, J. A BDOPV-Based Donor-Acceptor Polymer for High-Performance *n*-Type and Oxygen-Doped Ambipolar Field-Effect Transistors. *Adv. Mater.* **2013**, *25*, 6589–6593.
- (42) Yan, Z.; Sun, B.; Li, Y. Novel Stable (3E,7E)-3,7-Bis(2-oxoindolin-3-ylidene)benzo[1,2-*b*:4,5-*b'*]difuran-2,6(3H,7H)-dione Based Donor-Acceptor Polymer Semiconductors for *n*-Type Organic Thin Film Transistors. *Chem. Commun.* **2013**, *49*, 3790–3792.
- (43) Zhang, F.; Hu, Y.; Schuettfort, T.; Di, C.-A.; Gao, X.; McNeill, C. R.; Thomsen, L.; Mannsfeld, S. C. B.; Yuan, W.; Sirringhaus, H.; Zhu, D. Critical Role of Alkyl Chain Branching of Organic Semiconductors in Enabling Solution-Processed *n*-Channel Organic Thin-Film Transistors with Mobility of up to $3.50 \text{ cm}^2 \text{ V}^{-1} \text{ s}^{-1}$. *J. Am. Chem. Soc.* **2013**, *135*, 2338–2349.
- (44) Lee, J.; Han, A. R.; Yu, H.; Shin, T. J.; Yang, C.; Oh, J. H. Boosting the Ambipolar Performance of Solution-Processable Polymer Semiconductors via Hybrid Side-Chain Engineering. *J. Am. Chem. Soc.* **2013**, *135*, 9540–9547.
- (45) Meager, I.; Ashraf, R. S.; Mollinger, S.; Schroeder, B. C.; Bronstein, H.; Beatrup, D.; Vezie, M. S.; Kirchartz, T.; Salleo, A.; Nelson, J.; McCulloch, I. Photocurrent Enhancement from Diketopyrrolopyrrole Polymer Solar Cells through Alkyl-Chain Branching Point Manipulation. *J. Am. Chem. Soc.* **2013**, *135*, 11537–11540.